Journal of Geophysical Research: Biogeosciences

RESEARCH ARTICLE
10.1029/2017JG004288

Accumulation of Carbonates Contributes to Coastal Vegetated Ecosystems Keeping Pace With Sea Level Rise in an Arid Region (Arabian Peninsula)

Vincent Saderne[1], Michael Cusack[1], Hanan Almahasheer[2], Oscar Serrano[3], Pere Masqué[3,4,5], Ariane Arias-Ortiz[4], Periyadan Kadinjappalli Krishnakumar[6], Lotfi Rabaoui[6], Mohammad Ali Qurban[6,7], and Carlos Manuel Duarte[1]

[1]Red Sea Research Center, King Abdullah University of Science and Technology, Thuwal, Saudi Arabia, [2]Department of Biology, College of Science, Imam Abdulrahman Bin Faisal University, Dammam, Saudi Arabia, [3]School of Science and Centre for Marine Ecosystems Research, Edith Cowan University, Joondalup, Western Australia, Australia, [4]Institut de Ciència i Tecnologia Ambientals i Departament de Física, Universitat Autònoma de Barcelona, Bellaterra, Spain, [5]School of Physics and University of Western Australia Oceans Institute, University of Western Australia, Crawley, Western Australia, Australia, [6]Marine Studies Section, Center for Environment and Water, Research Institute, King Fahd University of Petroleum and Minerals, Dhahran, Saudi Arabia, [7]Geosciences Department, College of Petroleum Engineering and Geosciences, King Fahd University of Petroleum and Minerals, Dhahran, Saudi Arabia

Key Points:
- ^{210}Pb-20th century SARs in mangroves of Saudi Arabia are comparable to regional SLR, but not in salt marshes and seagrass meadows
- ^{14}C-centennial SARs in seagrass, mangrove, and saltmarsh ecosystems are of the order of 0.01 to 0.1 cm/year
- The SAR in tropical desert "blue carbon" ecosystems is supported by $CaCO_3$ accretion, comprising 40% to 60% of the soil volume

Supporting Information:
- Supporting Information S1
- Data Set S1
- Data Set S2

Correspondence to:
V. Saderne,
vincent.saderne@kaust.edu.sa

Citation:
Saderne, V., Cusack, M., Almahasheer, H., Serrano, O., Masqué, P., Arias-Ortiz, A., et al. (2018). Accumulation of carbonates contributes to coastal vegetated ecosystems keeping pace with sea level rise in an arid region (Arabian Peninsula). *Journal of Geophysical Research: Biogeosciences*, *123*. https://doi.org/10.1029/2017JG004288

Received 7 NOV 2017
Accepted 3 APR 2018
Accepted article online 12 APR 2018

Abstract Anthropogenic sea level rise (SLR) presents one of the greatest risks to human lives and infrastructures. Coastal vegetated ecosystems, that is, tidal marshes, seagrass meadows, and mangrove forests, elevate the seabed through soil accretion, providing a natural coastline protection against SLR. The soil accretion of these ecosystems has never been assessed in hot desert climate regions, where water runoff is negligible. However, tropical marine ecosystems are areas of intense calcification that may constitute an important source of sediment supporting seabed elevation, compensating for the lack of terrestrial inputs. We estimated the long-term (^{14}C-centennial) and short-term (^{210}Pb-20th century) soil accretion rates (SARs) and inorganic carbon (C_{inorg}) burial in coastal vegetated ecosystems of the Saudi coasts of the central Red Sea and the Arabian Gulf. Short-term SARs (±SE) in mangroves of the Red Sea (0.27 ± 0.22 cm/year) were twofold the SLR for that region since 1925 (0.13 cm/year). In the Arabian Gulf, only mangrove forest SAR is equivalent to local SLR estimates for the period 1979–2007 (0.21 ± 0.09 compared to 0.22 ± 0.05 cm/year, respectively). Long-term SARs are comparable or higher than the global estimates of SLR for the late Holocene (0.01 cm/year). In all habitats of the Red Sea and Arabian Gulf, SARs are supported by high carbonate accretion rates, comprising 40% to 60% of the soil volume. Further studies on the role of carbonates in coastal vegetated ecosystems are required to understand their role in adaptation to SLR.

Plain Language Summary Marine wetlands: mangroves, salt-marshes, and seagrass beds protect the coast against the human-induced sea level rise worldwide. They trap sediment, and this way elevated the seabeds, at paces equivalent to sea level rise. The amount of sediment trapped is generally linked to riverine inputs and surface runoff. However, in arid tropical regions, such as the Arabian peninsula, this source of sediment to the sea is almost unexistant. We studied the rate of seabed elevation in wetlands of the Red Sea and Arabian Gulf. We found that Mangrove and Seagrass (Red Sea only) seabed elevation rates are equivalent to sea level rise rates of the twentieth century, due to greenhouse gas emissions. This is possible because of accumulation of carbonate sediment coming from coral reefs weathering, replacing terrestrial inputs in the tropical arid area. Our study strengthens the relevance of wetlands to human societies in the mitigation of climate change, and we emphasize the need to protect and restore them.

1. Introduction

Accelerated ocean warming and ice melting resulting from anthropogenic climate change have doubled sea level rise (SLR) globally from about 0.17 cm/year for the period 1901–2010 to an average rate of about 0.32 cm/year for the period 1993–2010 (Church et al., 2013). Projections for the future are anticipating SLR rates peaking between 0.45 cm/year in 2050 (greenhouse gas concentration pathway "Representative Concentration Pathway [RCP]" 2.6) and 1.1 cm/year by the period 2081 to 2100 (RCP 8.5; Church et al., 2013). The global population at risk of flooding will increase in parallel, from about 189 million persons in

the year 2000 to up to 400 million by 2060 (Neumann et al., 2015), with severe socioeconomic impacts, particularly in tropical and subtropical coastal areas (Hallegatte et al., 2013; Neumann et al., 2015).

Coastal vegetated ecosystems—for example, tidal marshes, mangrove forests, and seagrass meadows—act as a natural protection against SLR, providing, if properly conserved or restored, an important element underpinning adaptation to SLR (Duarte et al., 2013; Societies & April, 2016). These ecosystems dissipate waves and currents and trap particles, thereby promoting the sedimentation and accretion of autochthonous and allochthonous material (Duarte et al., 2013). Soil accretion rates (SARs) in healthy coastal vegetated ecosystems are comparable to or exceed SLR, thereby countering marine transgression (Breithaupt et al., 2012; Kirwan et al., 2016; Mckee et al., 2007; Sanders et al., 2008, 2010, 2016; Sasmito et al., 2016). Globally, SARs average (±SE) 0.2 ± 0.04 cm/year in seagrass meadows (Duarte et al., 2013) and 0.51 ± 0.03 cm/year in tidal marshes (calculated from the supporting information of Kirwan et al., 2016, and only considering SAR derived from radiometric methods). In mangrove forests, Breithaupt et al. (2012) report a median (±SE of the median) SAR of 0.3 ± 0.4 cm/year. However, SAR differences between locations are large, depending on factors such as geomorphological settings, sedimentary riverine inputs, and hydrodynamic energy (e.g., Hayes et al., 2017; Serrano, Ruhon, et al., 2016).

Significant efforts have been devoted during the last decade to understand the role of coastal vegetated ecosystems as carbon sinks through burial of organic carbon, and thus their role in climate change mitigation through CO_2 sequestration (i.e., the blue carbon ecosystems concept; Duarte et al., 2013; McLeod et al., 2011; Nellemann et al., 2009). However, regarding SAR, organic carbon often only represents a small fraction of these soils (globally ~2–3% in seagrass and mangroves ecosystems; Fourqurean et al., 2012; Kristensen et al., 2008). Mineral deposits, siliciclastic and carbonate, generally account for the majority of the accreted substrate, contributing about 97–98% of the dry weight of seagrass and mangrove soils (Kristensen et al., 2008; Mazarrasa et al., 2015), and up to 50% in tidal marshes (Drake et al., 2015; Macreadie et al., 2013).

The accreted carbonate can originate from external sources: erosion of limestone and/or nearby habitats composed of carbonates (reefs and bioherms), and from autochthonous production by calcifying organisms inhabiting nearshore ecosystems (e.g., macroalgae, oysters, crabs, snails, and foraminifers; Por & Dor, 1975; Price et al., 1987, 1988; Sournia, 1977). Recently, Mazarrasa et al. (2015) estimated that the inorganic carbon (C_{inorg}, 12% of the calcium carbonate, $CaCO_3$, weight) burial rate in seagrass beds may reach 22 to 75 Tg C_{inorg}/year, mostly occurring in the intertropical areas (1.5% to 5% of the biogenic carbonate production of the global coastal ocean). These are regions of intense biomineralization by corals and algae, and in desert and semiarid climate regions, where terrigenous inputs are limited by the lack of surface runoffs, weathering of reefs and bioherms could be the principal source of sediment to the nearshore area. This suggests that in those regions, seabed elevation would be mainly supported by the accretion of carbonates.

The Arabian Peninsula is one of the driest areas of the planet, with precipitation less than 120 mm/year in 2016 (Global Precipitation Climatology Centre, accessed May 2017; Meyer-Christoffer et al., 2015). Terrigenous inputs of sediment are limited to airborne dust and rare surface water runoffs, with the exception of the Tigris and Euphrates Rivers (Al-Washmi, 1999; Basaham & El-Sayed, 1998; Behairy, 1980; El-Sayed, 1987; Pilkey & Noble, 1966).

In contrast, the Arabian Gulf and the Red Sea (Figure 1), flanking the Peninsula, are hot spots for carbonate production because their hypersaline and warm waters lead to high saturation states for carbonate minerals, thereby favoring biogenic carbonate deposition (Anderson & Dyrssen, 1994). In these desert environments, mangrove forests, tidal marshes, and seagrass meadows are the dominant vegetation in marine and terrestrial habitats.

The coastal area of the Arabian Peninsula is mostly composed by low-lying plains, both on the Red Sea and Arabian Gulf sides and is therefore vulnerable to SLR (Al-Jeneid et al., 2008; Alsahli & Al Hasem, 2016; Babu et al., 2012). Few tide gauge data exist for the Red Sea, and we are only aware of the estimate by Pugh and Abualnaja (2015) of a SLR rate of 0.13 cm/year over the period 1925–2013, from sporadic measurements in Port Soudan, slightly lower than the global SLR (0.17 cm/year; Church et al., 2013). The SLR in the western Arabian Gulf during the period 1979–2007 has been estimated at 0.22 ± 0.05 cm/year, based on data from seven tide gauges along the coast of Saudi Arabia (Alothman et al., 2014). This estimate is below the global estimate for the period 1993–2010 (0.32 cm/year; Church et al., 2013). However, a fraction of the SLR in the Arabian Gulf is attributed to land subsidence caused by groundwater pumping and oil extraction (0.07 cm/

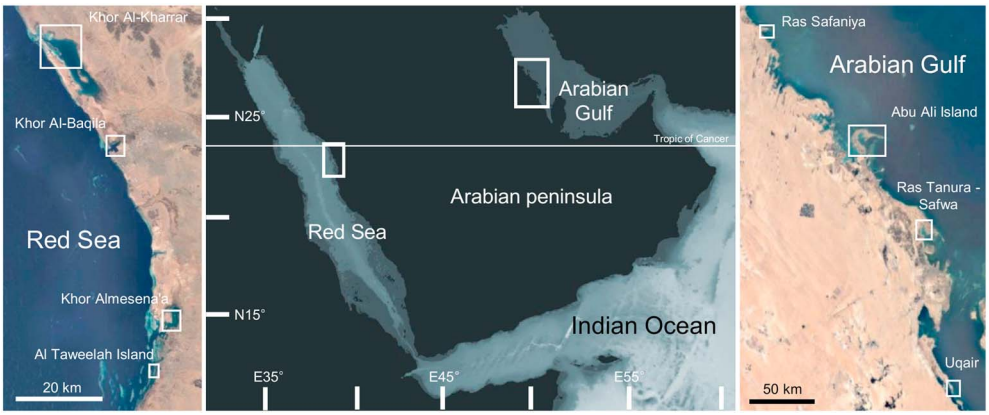

Figure 1. Locations of the coastal vegetated ecosystems sampled in the central Red Sea and Arabian Gulf. A detailed list of sampling sites is provided in the supporting information. Landsat/Copernicus satellite image.

year; Alothman et al., 2014). In that region, it is estimated that a 1-m SLR would flood approximately 1,200 km^2 of connected coastline of Kuwait, Saudi Arabia, and Bahrain (Al-Jeneid et al., 2008; Alsahli & Al Hasem, 2016; Babu et al., 2012). On the Red Sea side, the central coastal plain is experiencing rapid development and is therefore the most vulnerable zone to flooding with SLR (Hereher, 2016).

Hence, in this study, we quantify the SAR of mangroves forests, salt marshes ecosystems, and seagrass meadows in selected regions of the Arabian Peninsula that are vulnerable to SLR, the central Red Sea, and Arabian Gulf coasts. Furthermore, we evaluate the importance of carbonates in supporting the SAR in these desert climate ecosystems.

2. Materials and Methods

2.1. Ecosystem Description

Mangrove forests of the Red Sea and the Arabian Gulf are almost exclusively composed of *Avicennia marina* (although *Rhizophora mucronata* stands occur in few areas), generally a few meters in height and forming narrow coastal belts because of the limited tidal range (Almahasheer, Duarte, & Irigoien, 2016; Spalding et al., 2010). On the shores, the fossil coral flat bedrock is often located a few meters deep in the soil and emerges regularly at the surface (Behairy, 1983), leaving relatively shallow soils for mangroves to colonize. Hence, the mangroves of the Red Sea could be classified as soil starved, as observed in reef islands and other arid environments (Woodroffe et al., 2016). Tidal marshes of the Arabian coasts usually extend landward from the mangrove, occupying the high intertidal/low supratidal tidal zone. They are dominated by succulent shrubs species (e.g., *Suaeda vermiculata* and *Halopeplis perfoliata*), forming an ecosystem regionally known as "sabkha" (Ghazanfar, 2006) that occupies vast spans of coastal areas. Seagrass are present all along the Arabian coastline, with 12 species recorded in the Red Sea and 3 species in the Arabian Gulf (Green & Short, 2003). In contrast with global trends (Duarte et al., 2008), the areal coverage of mangroves and seagrass beds appears to be stable or even modestly expanding in the Red Sea (Almahasheer, Aljowair, et al., 2016; Price et al., 2014). Conversely, wetlands on the Saudi coast of the Arabian Gulf have been severely impacted (Almahasheer et al., 2013), with widespread losses due to land reclamation for residential, recreational, and industrial use (Sheppard et al., 2010). These ecosystems appear to be only remnants of what they once were but are now the subject of conservation efforts and revegetation by Arabian Gulf bordering countries.

2.2. Study Sites and Core Sampling

A total of 52 cores were sampled along 80-km coastline of the Kingdom of Saudi Arabia in the central Red Sea (2015) and the Arabian Gulf (2016; 29 in mangroves forests and 23 in seagrass meadows; Table 1). Seagrass soil cores were sampled in 1- to 4-m deep seagrass meadows, dominated by *Halophila* sp., *Thalassia hemprichii*, *Enhalus acoroides*, *Thalassodendrum ciliatum*, and *Cymodeacea* sp. Mangrove soil cores were sampled in intertidal monospecific *A. marina* forests. The sites sampled in the Red Sea include the nearshore island of Al Taweelah (22°16′N, 39°05′E; 8 mangrove and 3 seagrass coring locations) and 3 coastal lagoons: Khor

Journal of Geophysical Research: Biogeosciences

10.1029/2017JG004288

Table 1

Contemporary and Long-Term Soil Accumulation Rates (SARs), Inorganic Carbon Stocks (C_{inorg} in 1 m-Thick Sediments), and Short- and Long-Term Burial Rates in Coastal Vegetated Ecosystems of the Central Red Sea and Arabian Gulf Coasts of Saudi Arabia (Mean ± SE)

	Habitat	Location	Number of cores	$CaCO_3$ (%DW)	C_{inorg} stock (mg C_{inorg}/ha)	SAR ^{14}C (cm/year)	^{14}C slice age (year BP)	^{14}C dated slice depth (cm)	^{210}Pb SAR (cm/year)	^{210}Pb basal slice age (year Common Era)	^{14}C-derived C_{inorg} burial rate (g $C_{inorg} \cdot m^{-2} \cdot year^{-1}$)	^{210}Pb-derived C_{inorg} burial rate (g $C_{inorg} \cdot m^{-2} \cdot year^{-1}$)
Central Red Sea	Mangrove	Al Taweelah	8	97 ± 1	1200 ± 60	0.18 ± 0.35	2030 ± 450	67 ± 15	0.21 ± 0.07	1956 ± 6	170 ± 330	240 ± 80
		Khor Almesena'a	8	76 ± 2	820 ± 60	0.04 ± 0.01	2120 ± 370	77 ± 12			30 ± 10	
		Khor Al-Baqila	6	57	740	0.06 ± 0.02	2030 ± 620	84 ± 19	0.38 ± 0.16	1954 ± 20	45 ± 30	400 ± 170
		Khor Al-Kharrar	7	73 ± 7	860 ± 170	0.06 ± 0.06	1900 ± 490	68 ± 13	0.22 ± 0.22	1898 ± 74	50 ± 45	240 ± 230
	Seagrass	Al Taweelah	3	38 ± 12	380 ± 30	0.26 ± 0.15	780 ± 350	97 ± 37			90 ± 50	
		Khor Almesena'a	10	73 ± 4	730 ± 85	0.12 ± 0.12	980 ± 375	50 ± 8			90 ± 90	
		Khor Al-Kharrar	10	64 ± 3	620 ± 20	0.13 ± 0.07	470 ± 170	50 ± 11			100 ± 50	
	Mean	Mangrove		78 ± 4	890 ± 40	0.08 ± 0.17	2185 ± 280	74 ± 11	0.27 ± 0.22	1930 ± 35	80 ± 160	290 ± 120
		Seagrass		63 ± 4	570 ± 30	0.17 ± 0.11	880 ± 270	67 ± 28			90 ± 60	
Arabian Gulf	Mangrove	Abu Ali Island	3	39 ± 4	690 ± 80	0.07 ± 0.04	500 ± 300	34 ± 8	0.18 ± 0.07	1910 ± 10	60 ± 40	130 ± 80
		Ras Tanura-Safwa	4	79 ± 3	1350 ± 90	0.01 ± 0.001	2065 ± 130	22 ± 3	0.25 ± 0.09	1955 ± 10	10 ± 1	330 ± 120
	Seagrass	Abu Ali Island	3	67 ± 3	1000 ± 25	0.30 ± 0.15	280 ± 27	55 ± 14	0.13 ± 0.06	1850 ± 70	290 ± 40	120 ± 60
		Ras Tanura-Safwa	3	78 ± 1	1260 ± 70	0.11 ± 0.02	590 ± 160	51 ± 9	0.07 ± 0.03	1750 ± 120	130 ± 10	80 ± 25
		Ras Safaniya	3	50 ± 11	830 ± 205	0.06 ± 0.02	690 ± 270	42 ± 6	0.21 ± 0.05	1920 ± 15	50 ± 20	210 ± 40
		Uqair	3	52 ± 4	760 ± 20	0.31 ± 0.00	460 ± 40	33 ± 12	0.13 ± 0.04	1910 ± 6	240 ± 0.00	100 ± 30
	Sabkha	Abu Ali Island	3	48 ± 11	840 ± 120	0.05 ± 0.02	560 ± 320	28 ± 4	0.10 ± 0.02	1890 ± 10	40 ± 30	100 ± 25
		Ras Tanura-Safwa	3	66 ± 11	1100 ± 160	0.03 ± 0.01	680 ± 530	26 ± 6	0.09 ± 0.03	1900 ± 4	39 ± 18	100 ± 60
	Mean	Mangrove		62 ± 8	1012 ± 53	0.04 ± 0.04	1220 ± 430	28 ± 10	0.21 ± 0.09	1940 ± 10	35 ± 30	230 ± 180
		Seagrass		62 ± 4	960 ± 75	0.20 ± 0.11	665 ± 230	45 ± 11	0.13 ± 0.05	1860 ± 40	175 ± 90	130 ± 55
		Sabkha		57 ± 8	970 ± 110	0.04 ± 0.01	600 ± 270	27 ± 5	0.10 ± 0.01	1900 ± 5	40 ± 14	100 ± 15

Almesena'a (22°22′N, 39°07′E; 8 mangrove and 10 seagrass coring locations), Khor Al-Baqila (22°44′N, 39°00′E; 6 coring locations in mangroves), and Khor Al-Kharrar (22°57′N, 38°51′E; 7 coring locations in mangroves and 10 in seagrass beds; Figure 1). Khor Al-Baqila underwent a major alteration with the conversion of the entire southern side of the embayment into a petrochemical terminal starting in 1981. Similarly, an important development of hard engineering structures occurred in the shoreline in front of Al Taweelah Island in the early 2010s.

We also sampled 25 cores in the Saudi Arabian coast of the Arabian Gulf at four sites, Ras Safaniya (27°58′N, 48°46′E), Abu Ali Island (27°17′N, 49°33′E), Ras Tanura-Safwa (26°41′N, 50°00′E), and Uqair (25°43′N, 50°13′E; Figure 1). Three seagrass cores were sampled at each location in *Halodule uninervis* and *Halophila stipulacea* meadows (total of 12 cores). Additionally, three mangrove and three sabkha cores were sampled in the south of Abu Ali Island and four mangrove cores and three sabkha cores were sampled in the area of Ras Tanura-Safwa (Figure 1). All sites except Uqair have undergone alterations associated with the prevalent industrial and urban development in the region since the 1950s, including land reclamation, construction of bridges and pipelines, dredging, and oil spills.

Soil cores were sampled using manual percussion and rotation (polyvinyl chloride pipe with an inner diameter of 70 mm). The length of core barrel inserted into the soil and the length of retrieved soil were recorded in order to correct for compression effects following the guidelines of Howard et al. (2014). All variables studied here are referenced to the corrected, uncompressed depths. The cores were sealed at both ends, transported vertically, and stored at 4°C before processing in the laboratory.

2.3. Biogeochemical Analysis

The soil cores were segmented into 1-cm-thick slices, which were oven-dried at 60°C until constant weight to determine the dry bulk density (DBD; g/cm^3). The slices were then ground in an agate mortar and subdivided for analysis. All depths were corrected for compression considering a uniform distribution of the compaction throughout the total length of the cores as described by Serrano, Ricart, et al. (2016). The mean ± SE compression factors (depth ratios between compressed and uncompressed soils) were 1.05 ± 0.18, 1.04 ± 0.03, and 1.16 ± 0.11 in the cores from sabkha, mangrove, and seagrass sites of the Arabian Gulf, respectively, and 1.19 ± 0.14 and 1.23 ± 0.17 in the seagrass and mangrove cores of the Red Sea.

Short-term (last decades to century) and long-term (millennia) soil chronologies were established using ^{210}Pb and ^{14}C analyses, respectively. Forty-five cores were analyzed to retrieve chronologies using the ^{210}Pb technique, 20 cores from the Red Sea (9 in seagrass and 11 in mangroves), and 25 cores from the Arabian Gulf (7 in mangroves, 12 in seagrass, and 6 in sabkhas). The activity concentrations of ^{210}Pb in the upper 20 to 30 cm were determined in the soil fraction $<$0.125 mm by alpha spectrometry through the measurement of its granddaughter ^{210}Po, assuming radioactive equilibrium between both radionuclides (Sanchez-Cabeza et al., 1998). The activity concentrations of excess ^{210}Pb used to obtain the age models were determined as the difference between total ^{210}Pb and ^{226}Ra (supported ^{210}Pb). Concentrations of ^{226}Ra were determined for selected samples along each core by low-background liquid scintillation counting method (Wallac 1220 Quantulus) adapted from Masqué et al. (2002). These activity concentrations were found to be comparable with the concentrations of total ^{210}Pb at depth below the excess ^{210}Pb horizons. Analyses of reagent blanks, replicates, and a reference material (IAEA-315, marine soils) were carried out for both ^{210}Pb and ^{226}Ra to assess for any contamination and to ensure reproducibility of the results. Average soil mass accumulation rates (MARs, expressed in g DW $\cdot$ cm^{-2} $\cdot$ year^{-1}) for the last decades/century were estimated using the constant flux:constant sedimentation model (Krishnaswamy et al., 1971). MARs were transformed into SAR (cm/year) using the DBD of each core.

A total of 179 radiocarbon analyses were conducted in 77 cores (25 cores from the Arabian Gulf and 52 from the Red Sea) by accelerator mass spectrometry. Analyses were done at two soil depths per core in the Red Sea cores and three depths in the Arabian Gulf cores, following standard procedures (ISO 17025 and ISO 9001) at the AMS Direct Laboratory, United States. Samples consisted of either pooled shells or bulk soils. The raw radiocarbon dates reported by the laboratory were calibrated using the R routine "Bacon" for Bayesian chronology building (Blaauw & Christeny, 2011), assuming marine reservoir corrections of 110 ± 38 and 180 ± 53 years for the Red Sea and the Arabian Gulf, respectively (Southon et al., 2002). From the Bacon routine output, the mean age was used to produce an age-depth weighted regression model forced through 0

(0 cm is 1950 B.P.), using as weight the sum of the Euclidean distances of the minimum and maximum ages. We report the slope ± SE of the regression as the corresponding long-term SAR.

2.4. Carbonate Content and C_{inorg} Burial Rates

Calcium carbonate ($CaCO_3$) content was determined in every fourth to fifth centimeter from surface to 20-cm depth. $CaCO_3$ measurements were done with a calcimeter (Pressure Gauge Model 432, Fann, Houston, TX, United States; ASTM D 4373-84 Standard) by reacting the $CaCO_3$ present in the sample with 10% HCl in a sealed reaction cell. The pressure build up due to the CO_2 was measured with a bourdon tube pressure gauge that was precalibrated with reagent grade $CaCO_3$.

Calcium carbonate densities per unit area (g $CaCO_3/cm^3$) were calculated by multiplying the soil DBD (g/cm^3) by the $CaCO_3$ content (%). The $CaCO_3$ accumulation rates ($g\ CaCO_3 \cdot m^{-2} \cdot year^{-1}$) were calculated by multiplying the mean $CaCO_3$ densities throughout the 20 first centimeters by the soil accumulation rates ($g \cdot m^{-2} \cdot year^{-1}$) derived from both ^{210}Pb and ^{14}C age-depth models. Twenty centimeters was the depth encompassed by all cores, thereby allowing intercomparison without requiring extrapolations.

In the Arabian Gulf cores, the theoretical contribution of $CaCO_3$ to the SAR (in cm/year) was estimated as the sum of the volume occupied by pure theoretical calcium carbonate crystals (calcite and aragonite) and the interstitial volume between and within $CaCO_3$ grains, that is, porosity (P). The porosity of the soil, in percent of soil volume, was estimated from the weight of water in the soil:

$$P = \frac{(WW_{soil} - DW_{soil}) \times \rho_w}{V_{soil}} \times 100$$

where WW_{soil} and DW_{soil} are the dry and wet weights of a given slice in grams, ρ_w is the density of water (we used $\rho_w = 1\ g/cm^3$), and V_{soil} is the volume of soil in the slice (decompressed).

The volume occupied by the theoretical, pure $CaCO_3$ crystal fraction of the soil (V_p in cm^3 g/soil) was estimated as

$$V_p = \frac{DW_{carb}}{100} \times \frac{1}{\rho_{carb}}$$

where DW_{carb} is the $CaCO_3$ content (% of soil DW) and $\rho_{carb} = 2.7\ g/cm^3$ is the mean density of calcite and aragonite crystals (Reghellin et al., 2013).

The theoretical volume occupied by carbonate grains in the sediment (V_{carb} in cm^3 g/soil) was estimated as the volume of $CaCO_3$ crystals and the space between and within $CaCO_3$ grains:

$$V_{carb} = \frac{P}{100} \times Vp + Vp$$

The contribution of $CaCO_3$ to the SAR was then calculated as the mean V_{carb} in the upper 20 first centimeter multiplied by the MAR derived from the ^{210}Pb and ^{14}C dating age models. The long-term C_{inorg} burial rates of ^{14}C is therefore an estimate based on the average $CaCO_3$ content of the upper 20 first centimeter, assuming that this average remains constant with depth.

The wet weight of soil was not measured during the Red Sea sampling campaign of 2015, and thus, the calculations were done using core average values (from surface to 20 cm compressed), and the average porosities from the Arabian Gulf seagrasses and mangroves cores (34% and 36%, respectively).

The complete data sets, including ^{14}C and ^{210}Pb data, $CaCO_3$ concentration values, porosities and $CaCO_3$ depth profiles for all cores, are available in the supporting information and from the open repository Pangaea (Saderne et al., 2018).

3. Results

3.1. ^{210}Pb-Contemporary Sedimentation Rates (20th and 21st Centuries)

In the Red Sea, 9 and 11 cores were analyzed for ^{210}Pb in seagrass and mangrove ecosystems, respectively. Of these, only four mangrove cores presented an excess ^{210}Pb profile allowing short-term SAR determinations,

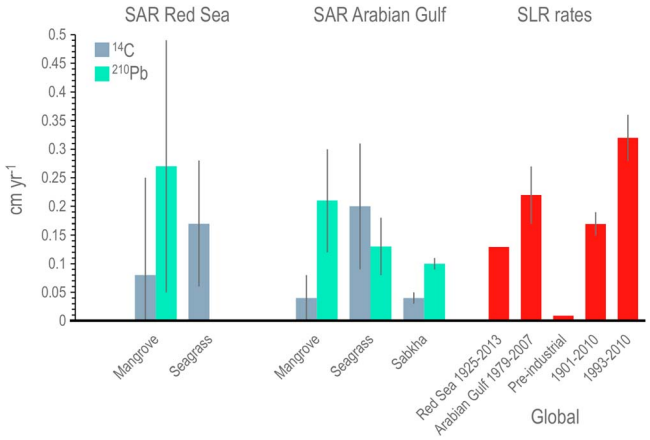

Figure 2. Mean (±SE) soil accretion rates (SARs) in coastal ecosystems of the Arabian Peninsula compared to regional and global sea level rise (SLR) rates, in cm/year. In gray long-term (^{14}C) rates, in green contemporary (^{210}Pb) SAR.

averaging (± SE) 0.27 ± 0.22 cm/year (Table 1 and Figure 2). The ^{210}Pb data of all the other cores suggested an absence of net soil accretion or intense soil reworking during the last decades/century.

Of the 25 cores of the Arabian Gulf analyzed for ^{210}Pb, 4 cores did not present any excess ^{210}Pb, and thus, an age model could not be produced. The activity concentrations of excess ^{210}Pb decreased steadily from surface to the excess ^{210}Pb horizon in four mangrove cores and one sabkha core. In the other Arabian Gulf cores, the ^{210}Pb concentrations profiles in mangrove forests and sabkhas showed evidence of mixing in the upper 5 and 3 cm (on average), respectively (supporting information). In seagrass soils, the thickness of the mixed layer varied from 6 to 12 cm. Mixing may contribute to the overestimation of SAR estimates by ^{210}Pb (Cochran, 1985; Nittrouer et al., 1984); hence, short-term SAR should be considered as upper limits. One core could not be dated with either ^{210}Pb or ^{14}C techniques.

The mean ± SE short-term SAR in the Arabian Gulf are 0.21 ± 0.09, 0.13 ± 0.05, and 0.10 ± 0.01 cm/year for mangrove, seagrass, and sabkha ecosystems, respectively (Table 1 and Figure 2). The short-term SARs range from 0.12 ± 0.01 to 0.36 ± 0.04 cm/year in the mangrove forests, from 0.06 ± 0.02 to 0.24 ± 0.03 cm/year in seagrass meadows, and from 0.06 ± 0.01 to 0.13 ± 0.01 cm/year in sabkhas (mean ± SE; see supporting information).

3.2. ^{14}C-Centennial Sedimentation Rates

In the Red Sea, cores from 29 mangrove forests and 22 seagrass meadows were dated with ^{14}C. Of those, five mangrove and two seagrass cores did not return a coherent geochronology. The long-term SARs derived from ^{14}C in mangrove forests and seagrass meadows are 0.08 ± 0.17 and 0.17 ± 0.11 cm/year, respectively (mean ± SE; Table 1 and Figure 2).

Of the 25 cores sampled from the Saudi coast of the Arabian Gulf, all were dated with ^{14}C, but 7 yielded incoherent geochronologies (i.e., reversals) and 2 cores could not be dated (modern soils). The average ^{14}C-derived SARs for mangrove, seagrass, and sabkha ecosystems for the last 2,000 years are 0.04 ± 0.04, 0.20 ± 0.11, and 0.04 ± 0.01 cm/year, respectively (mean ± SE; Table 1 and Figure 2).

3.3. Contribution of Carbonates to Soil Accretion

The SAR in all habitats in the Red Sea and Arabian Gulf are mostly supported by carbonates, which accounts for 65 ± 8% and 60 ± 2% of the soil dry weight along the upper 20 cm, respectively.

Converted into inorganic carbon, we estimate a short-term burial rate in the Red Sea mangroves of 290 ± 120 g $C_{inorg} \cdot m^{-2} \cdot year^{-1}$ (mean ± SE). In the mangrove forests, seagrass meadows, and sabkhas of the Arabian Gulf, the short-term burial rates of C_{inorg} are 230 ± 180, 130 ± 55, and 100 ± 15 g $C_{inorg} \cdot m^{-2} \cdot year^{-1}$, respectively (mean ± SE; Table 1 and Figure 3). The long-term burial rates in the mangrove forests of the Red Sea and the Arabian Gulf are 80 ± 160 and 35 ± 30 g $C_{inorg} \cdot m^{-2} \cdot year^{-1}$, respectively (mean ± SE; Table 1 and Figure 3). The long-term burial rates of C_{inorg} in the Red Sea and Arabian Gulf seagrass meadows are 90 ± 60 and 175 ± 90 g $C_{inorg} \cdot m^{-2} \cdot year^{-1}$ (mean ± SE; Table 1 and Figure 3).

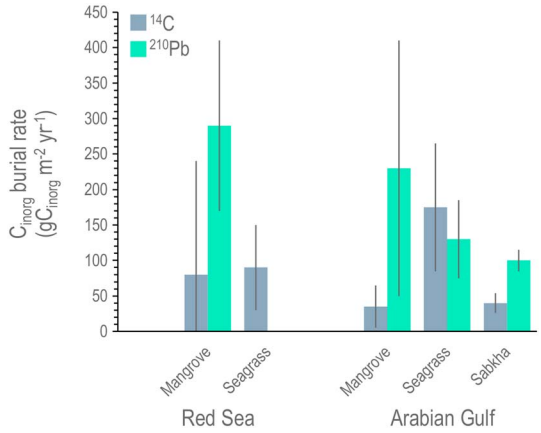

Figure 3. Mean (±SE) inorganic carbon (C_{inorg}) burial rates in coastal ecosystems of the Arabian Peninsula. In gray long-term (^{14}C) rates, in green contemporary (^{210}Pb) soil accretion rates.

The mean (±SE) short-term vertical accretions due to $CaCO_3$ in the Arabian Gulf seagrass meadows, mangroves, and sabkhas are 0.08 ± 0.01, 0.13 ± 0.03, and 0.05 ± 0.01 cm/year (54, 57, and 50%vol of the SAR, respectively). The short-term accretion of $CaCO_3$ in the Red Sea mangroves is estimated to be 0.15 ± 0.05 cm/year (mean ± SE; 60%vol of the SAR). It was not possible to estimate short-term accretion rates with ^{210}Pb for Red Sea seagrass ecosystems (see above). However, the long-term $CaCO_3$ accretion in the Red Sea seagrass meadows is 0.06 ± 0.01 cm/year (mean ± SE; 40%vol of the SAR).

4. Discussion

4.1. Contemporary Rates

The results obtained show that the Red Sea mangrove ecosystems accrete soils at a rate up to twofold higher (0.27 ± 0.22 cm/year) than the SLR estimates for the last century (0.13 cm/year; Pugh & Abualnaja, 2015; Figure 2) We could not obtain a short-term SAR estimate for the Red Sea seagrass ecosystems; however, the long-term SAR of 0.17 ± 0.11 suggests that they may have been able to keep pace with SLR over the past century.

In the Arabian Gulf, however, only mangroves accreted soils during the twentieth century at a rate (0.21 ± 0.09 cm/year) equivalent to SLR estimates for the period 1979–2007 (0.22 ± 0.05 cm/year; Alothman et al., 2014; Figure 2). Short-term SAR in sabkhas and seagrass meadows are about half of the SLR estimates. In the current state, the contemporary SAR supported by marine vegetated ecosystems of the Saudi coast are insufficient to counter future SLR rates predicted under the most optimistic RCP scenario (RCP 2.6, up to 0.45 cm/year; Church et al., 2013). Moreover, the difference between SAR supported by Arabian Gulf ecosystems and projected SLR may be widened further by land subsidence in the Arabian Gulf.

The contemporary SAR estimated for seagrass meadows of the Arabian Gulf (0.13 ± 0.05 cm/year) is almost 3 times lower than the SAR estimated for seagrass meadows globally (0.35 ± 0.06 cm/year; Table 2). Likewise, the short-term SAR for sabkhas in the Arabian Gulf (mean ± SE of 0.10 ± 0.01) is lower than the published short-term SAR rates in temperate tidal marshes, which range from 0.1 to 1.4 cm/year, with a mean (±SE) of 0.51 ± 0.03 cm/year (data retrieved from Kirwan et al., 2016).

In mangrove forests, our estimates of the median contemporary SAR compare well with the global median estimate by Breithaupt et al. (2012) of 0.3 ± 0.4 cm/year, with 0.29 ± 0.28 and 0.20 ± 0.12 cm/year in the Red Sea and Arabian Gulf, respectively (median ± SE of the median). However, almost all study sites in Breithaupt et al. (2012) are located in estuaries or coastal areas with riverine inputs and/or in regions with higher precipitation regimes than in the Arabian Peninsula, which likely supports SAR through inputs of allochthonous particles.

4.2. Centennial Rates

The long-term SARs in coastal vegetated ecosystems of the Arabian Peninsula are of the order of 0.01 to 0.1 cm/year. When compared to global SLR estimated over preindustrial periods by the Intergovernmental Panel on Climate Change (about 0.01 cm/year; Church et al., 2013), this suggests that these ecosystems kept pace with SLR over centuries to millennia. In the case of mangrove forests, similar trends are observed in Singapore, Southeast Australia, or the Caribbean area (Bird et al., 2004; Hashimoto et al., 2006; Mckee et al., 2007). As an example, in Caribbean mangroves, Mckee et al. (2007) determined a SAR of approximately 0.1 cm/year for the period 2000–400 calibrated year B.P. in parallel with mangrove SLR rates of 0.09 cm/year.

A total of 14 cores were dated using both ^{14}C and ^{210}Pb methods. Long-term SAR is statistically larger than the short-term SAR in only two of them, with a mean (±SE) difference of 0.13 ± 0.05 cm/year (95% CI of 0.11). As a general trend, estimates of long-term SAR derived from ^{14}C in soils are lower than short-term SAR derived from ^{210}Pb (Baskaran et al., 2016). For example, Serrano, Ruhon, et al. (2016), Serrano, Ricart, et al. (2016) reported ^{14}C-based SAR 1.2 to 4 times less than ^{210}Pb-based SAR (Table 2). Discrepancies between ^{14}C- and ^{210}Pb-based SAR are also reported in unvegetated soils (Baskaran et al., 2016). According to Baskaran et al. (2016), the reasons for this difference could be due to (1) errors in short-term dating due to reworking of the soil by anthropogenic activities (secondary deposition) or bioturbation, (2) errors in long-term estimates due to loss of volume at depth (i.e., compaction and long-term remineralization), and (3) underestimates of the reservoir effect (^{14}C).

Accordingly, the apparent acceleration of soil accretion in coastal ecosystems of the Arabian Peninsula could be artefactual or be linked to sediment reworking due to land-based anthropogenic activities or dredging. It could, however, also be a consequence of recent acceleration of SLR.

4.3. Contribution of Carbonates to Soil Accretion

Seabed elevation in the Arabian Peninsula's coastal vegetated habitats is mostly supported by carbonates, in both weight and volume. On average, $CaCO_3$ represents 54% (ranging from 20% to 80%) of the soil volume in the Red Sea and Arabian Gulf nearshore ecosystems.

Table 2
Published ^{14}C (Long-Term) and ^{210}Pb (Short-Term) Soil Accumulation Rates (SARs) in Seagrass Meadows

Location	^{14}C-based SAR (cm/year)	^{14}C age interval (year B.P.)	^{210}Pb-based SAR (cm/year)	Source
Rottnest Isl., Australia	0.13 ± 0.01	498	0.30 ± 0.11	Serrano, Ruhon, et al. (2016)
	0.15 ± 0.01	485	0.20 ± 0.07	
	0.08 ± 0.003	490	0.16 ± 0.07	
	0.11 ± 0.004	497	0.13 ± 0.02	
Cockburn Sound, Australia	0.044 ± 0.005	511–3132	0.178 ± 0.007	Serrano, Ricart, et al. (2016)
Oyster Harbor, Australia			0.25 ± 0.01	Serrano, Davis, et al. (2016)
			0.27 ± 0.08	
Oyster Harbor, Australia			0.103 ± 0.008	Marbà et al. (2015)
Gulf of Mexico, Mexico			0.4	Gonneea et al. (2004)
			0.15	
			0.2	
Chesapeake Bay, USA			1	Palinkas & Koch (2012)
			1.28	
			0.92	
			0.39	
			0.22	
Atlantic Ocean, USA			0.66	Greiner et al. (2013)
Puget Sound, United States			0.18	Poppe (2015)
			0.2	
			0.079	
			0.24	
			0.21	
			0.49	
Baltic Sea, Poland			0.13 ± 0.02	Jankowska et al. (2016)
Ischia Isl., Italy	0.165	525–1755		Mateo et al. (1997)
Gulf of Lion, Spain	0.061	735–2190		
	0.414	450–825		
	0.079	1260–3180		
SW Mediterranean Sea, Spain	0.203	525–1350		
	0.114	195–1305		
	0.188	150–480		
Gulf of Lion, Spain	0.11	1441–5616		Lo Iocano et al. (2008)
Gulf of Lion, Spain	0.13	710–3850		Serrano et al. (2012)
Jervis Bay, Australia	0.015	6255–6476		Macreadie et al. (2015)
	0.017	228–5232		
	0.028	168–2115		
Seto Inland Sea, Japan	0.037 ± 0.001	535–5585		Miyajima et al. (2015)
	0.099 ± 0.009	2000–2790		
	0.134 ± 0.016	1265–2035		
Ishikagi Isl., Japan,	0.123 ± 0.01	310–870		
Adaman Sea, Thailand	0.081 ± 0.002	343–2150		
Mean ± SE	0.12 ± 0.02		0.35 ± 0.06	

In seagrass meadows, Mazarrasa et al. (2015) calculated a global mean C_{inorg} stock (within the top 1 m of soil) of 654 ± 24 Mg C_{inorg}/ha (ranging between 3 and 1,660 Mg C_{inorg}/ha). The C_{inorg} stocks in seagrass meadows of the Red Sea and Arabian Gulf are comparable to this global estimate, 570 ± 30 and 960 ± 75 Mg C_{inorg}/ha, respectively (mean ± SE; Table 1).

A global burial rate of 126 ± 31 g $C_{inorg} \cdot m^{-2} \cdot year^{-1}$ in seagrass meadows was indirectly calculated from global averages of SAR and C_{inorg} density (Mazarrasa et al., 2015). The long- and short-term burial rates of C_{inorg} in the Arabian Gulf seagrass meadows are also similar to this global estimate, with 175 ± 90 and 130 ± 55 g $C_{inorg} \cdot m^{-2} \cdot year^{-1}$, respectively. In the Red Sea meadows, however, the long-term burial rates are lower than the global estimate, with 90 ± 60 g $C_{inorg} \cdot m^{-2} \cdot year^{-1}$.

Brunskill et al. (2002) measured the contemporary organic and inorganic carbon burial rates on the Great Barrier Reef continental shelf (North Queensland, Australia), on transects from the mangrove forest to the reef and the shelf slope. Located in an area of tropical wet climate and in the plume of a river, the mangrove soils comprise less than 10% DW of $CaCO_3$ and a mean (±SE) C_{inorg} burial rate of 11 ± 6 g $C_{inorg} \cdot m^{-2} \cdot year^{-1}$. This

value is 1 order of magnitude lower than in the Arabian Peninsula, despite the proximity of the Great Barrier Reef (where they estimated C_{inorg} burial rates of 430 g $C_{inorg} \cdot m^{-2} \cdot year^{-1}$). The difference between our results in the dry tropics and the results of Brunskill et al. (2002) in the wet tropics illustrates that the accumulation of carbonates of marine origin plays an important role in seabed elevation in the absence of surface runoff.

To our knowledge, this is the first paper that directly assesses burial rates of inorganic carbon in tidal marshes (or sabkhas here).The marine soils of the Saudi coasts of the Red Sea and the Arabian Gulf are mostly composed of aragonite and magnesium-rich calcite, pointing to a recent biogenic origin from coral reefs, echinoderms, and coralline algae (Al-Washmi, 1999; Behairy, 1980; Pilkey & Noble, 1966). In our study, we found high percentages of $CaCO_3$ in sabkhas (57 ± 8% DW). These ecosystems do not host any important calcifying fauna or flora, and most of the carbonates present in the soil are imported from nearby marine ecosystems, as shown by Khalaf and Ala (1980). We do not currently have estimates on local production of $CaCO_3$ by organisms inhabiting seagrass beds, mangroves, and sabkhas of the Red Sea and the Arabian Gulf. This limits our capacity to evaluate the importance of in situ calcification in supporting the SAR (Macreadie et al., 2017). To our knowledge, there are no published estimates of calcification by associated biota in mangrove forests or tidal marshes. However, regarding seagrass meadows, calcification rates by associated organisms are of the order of 10 g $C_{inorg} \cdot m^{-2} \cdot year^{-1}$ in tropical areas (James et al., 2009). This is approximately 1 order of magnitude lower than the burial rates of C_{inorg} in the seagrass soils of our study. This discrepancy support the hypothesis that carbonates may largely be of allochthonous origin, primarily imported from adjacent coral reefs. Likewise, as an argument in the sense of a low contribution of associated organisms' calcification to sediment composition, Mazarrasa et al. (2015) noted that, globally, seagrass meadows and adjacent unvegetated areas have similar inorganic carbon density.

Whereas calcification in vegetated ecosystems may play a role in supporting SAR, it also affects their role as CO_2 sinks (Pergent et al., 2012). Calcification emits CO_2 with a ratio of approximately 0.6 mol of CO_2 emitted per mol of $CaCO_3$ precipitated (Ware et al., 1992), since the consumption of total alkalinity (Ca^{2+}) exceeds the consumption of dissolved inorganic carbon. When $CaCO_3$ redissolves, the CO_2 emitted during calcification is taken up again through the release of the sequestrated alkalinity. The high amount of carbonates in blue carbon ecosystems soils may be an indicator of intense local calcification activity and CO_2 release, countering the CO_2 uptake by organic carbon sequestration (Macreadie et al., 2017). However, the assumption that the carbonate stocks in the soils are partially or largely allochthonous makes it impossible to use the carbonate burial rates to estimate the CO_2 emissions due to calcification. Doing so as an attempt to obtain the net CO_2 balance of blue carbon ecosystems would lead to overestimates and potentially flawed CO_2 budgets (Macreadie et al., 2017).

5. Conclusion

Our results suggest that mangrove forests and seagrass meadows in the Saudi coast of the central Red Sea have supported SAR at a pace equivalent to SLR over the past millennia and at least comparable to SLR over the last century. In the Arabian Gulf, however, only mangrove forests seem to keep pace with the high contemporary SLR resulting from the combined effects of global anthropogenic climate change and regional land subsidence. In contrast to the Red Sea (Almahasheer, Aljowair, et al., 2016), nearshore vegetated ecosystems in the Arabian Gulf have been massively destroyed by urbanization and industrial activities over the past decades (Sheppard et al., 2010). The loss of coastal wetlands reduces coastal protection, further aggravating risks from SLR. The contribution of carbonates to both short- and long-term SAR is key in the maintenance of the seabed elevation rates to keep pace with SLR in arid and semiarid tropical area. However, the dissolution rates of marine carbonate sediments could increase in the future as the corrosiveness of seawater for carbonates increases due to climate change and ocean acidification (increase of CO_2 concentrations in seawater; Eyre et al., 2014).

Acknowledgments
This research was supported by a project funded by Saudi Aramco and baseline funding from King Abdullah University of Science and Technology (KAUST). O. S. was supported by an ARC DECRA (DE170101524). Funding was provided to PM by the Generalitat de Catalunya (grant 2014 SGR-1356) and an Australian Research Council LIEF Project (LE170100219). AAO was supported by a PhD scholarship from Obra Social "LaCaixa". This work is contributing to the ICTA 'Unit of Excellence' (MinECo, MDM2015-0552). We thank A. Qasem and P. Priahartato, Saudi Aramco, for support and advice on sampling design; R. Lindo, R. Magalles, P. Bacquiran, S. Ibrahim, and M. Lopez, at the Marine Studies section of the Center for Environment and Water of King Fahd University of Petroleum and Minerals; and Z. Batang and staff from the Coastal and Marine Resources core lab at KAUST for help with sampling. We thank I. Schulz, N. Geraldi, K. Rowe, S. Roth, M. Ennasri, D. Prabowo, and I. Mendia for help with laboratory analyses. We wish to thank the two anonymous reviewers, as well as Editor in chief M. Goni, for their precious comments/suggestions for the improvement of the manuscript. The data sets, including ^{14}C and ^{210}Pb data, $CaCO_3$ concentration values, porosities, and $CaCO_3$ depth profiles for all cores, are available in the open repository Pangaea (Saderne et al., 2018; https://doi.pangaea.de/10.1594/PANGAEA.887043).

References

Al-Jeneid, S., Bahnassy, M., Nasr, S., & El Raey, M. (2008). Vulnerability assessment and adaptation to the impacts of sea level rise on the Kingdom of Bahrain. *Mitigation and Adaptation Strategies for Global Change*, *13*(1), 87–104. https://doi.org/10.1007/s11027-007-9083-8

Almahasheer, H., Aljowair, A., Duarte, C. M., & Irigoien, X. (2016). Decadal stability of Red Sea mangroves. *Estuarine, Coastal and Shelf Science*, *169*, 164–172. https://doi.org/10.1016/j.ecss.2015.11.027

Almahasheer, H., Al-Taisan, W., & Mohamed, M. K. (2013). Mangrove deterioration in Tarut Bay on the Eastern Province of the Kingdom of Saudi Arabia. *Pakhtunkhwa Journal of Life Science*, *02*, 49–59.

Almahasheer, H., Duarte, C. M., & Irigoien, X. (2016). Nutrient limitation in central Red Sea mangroves. *Frontiers in Marine Science*, *3*. https://doi.org/10.3389/fmars.2016.00271

Alothman, A. O., Bos, M. S., Fernandes, R. M. S., & Ayhan, M. E. (2014). Sea level rise in the north-western part of the Arabian Gulf. *Journal of Geodynamics*, *81*, 105–110. https://doi.org/10.1016/j.jog.2014.09.002

Alsahli, M. M. M., & Al Hasem, A. M. (2016). Vulnerability of Kuwait coast to sea level rise. *Geographical Tidsskrift Journal Geographical*, *116*(1), 56–70. https://doi.org/10.1080/00167223.2015.1121403

Al-Washmi, H. A. (1999). Sedimentological aspects and environmental conditions recognized from the bottom sediments of Al-Kharrar lagoon, eastern Red Sea coastal plain, Saudi Arabia. *Journal King Abdulaziz University Science*, *10*(1), 71–87. https://doi.org/10.4197/mar.10-1.5

Anderson, L., & Dyrssen, D. (1994). Alkalinity and total carbonate in the Arabian Sea. Carbonate depletion in the Red Sea and Persian Gulf. *Marine Chemistry*, *47*(3–4), 195–202. https://doi.org/10.1016/0304-4203(94)90019-1

Babu, D. S. S., Sivalingam, S., & Machado, T. (2012). Need for adaptation strategy against global sea level rise: An example from Saudi coast of Arabian Gulf. *Mitigation and Adaptation Strategies for Global Change*, *17*(7), 821–836. https://doi.org/10.1007/s11027-011-9346-2

Basaham, A. S., & El-sayed, M. A. (1998). Distribution and phase association of some major and trace elements in the Arabian Gulf sediments. *Estuarine, Coastal and Shelf Science*, *46*(2), 185–194. https://doi.org/10.1006/ecss.1997.0278

Baskaran, M., Bianchi, T. S., & Filley, T. R. (2016). Inconsistencies between ^{14}C and short-lived radionuclides-based sediment accumulation rates: Effects of long-term remineralization. *Journal of Environmental Radioactivity*, *174*, 10–16. https://doi.org/10.1016/j.jenvrad.2016.07.028

Behairy, A. K. A. (1980). Clay and carbonate mineralogy of the reef sediments north of Jeddah, west coast of Saudi Arabia. *Bulletin of Faculty Science King Abdulaziz University*, *4*, 265–279.

Behairy, A. K. A. (1983). Marine transgressions in the west coast of Saudi Arabia (Red Sea) between mid-Pleistocene and present. *Marine Geology*, *52*(1–2), M25–M31. https://doi.org/10.1016/0025-3227(83)90016-6

Bird, M. I., Fifield, L. K., Chua, S., & Goh, B. (2004). Calculation sediment compacting for radiocarbon dating of intertidal sediments. *Radiocarbon*, *46*(01), 421–435. https://doi.org/10.1017/S0033822200039734

Blaauw, M., & Christeny, J. A. (2011). Flexible paleoclimate age-depth models using an autoregressive gamma process. *Bayesian Analysis*, *6*(3), 457–474. https://doi.org/10.1214/11-BA618

Breithaupt, J. L., Smoak, J. M., Smith, T. J., Sanders, C. J., & Hoare, A. (2012). Organic carbon burial rates in mangrove sediments: Strengthening the global budget. *Global Biogeochemical Cycles*, *26*, GB3011. https://doi.org/10.1029/2012GB004375

Brunskill, G. J., Zagorskis, I., & Pfitzner, J. (2002). Carbon burial rates in sediments and a carbon mass balance for the Herbert River region of the Great Barrier Reef Continental Shelf, North Queensland, Australia. *Estuarine, Coastal and Shelf Science*, *54*(4), 677–700. https://doi.org/10.1006/ecss.2001.0852

Church, J. A., Clark, P. U., Cazenave, A., Gregory, J. M., Jevrejeva, S., Levermann, A., et al. (2013). Sea level change. In T. F. Stocker, et al. (Eds.), *Climate change 2013: The physical science basis. Contribution of working group I to the Fifth Assessment Report of the Intergovernmental Panel on Climate Change* (pp. 1137–1216). Cambridge, UK and New York: Cambridge University Press. https://doi.org/10.1017/CB09781107415315.026

Cochran, J. K. (1985). Particle mixing rates in sediments of the eastern equatorial Pacific: Evidence from ^{210}Pb, $^{239,240}Pu$ and ^{137}Cs distributions at MANOP sites. *Geochimica et Cosmochimica Acta*, *49*(5), 1195–1210. https://doi.org/10.1016/0016-7037(85)90010-9

Drake, K., Halifax, H., Adamowicz, S. C., & Craft, C. (2015). Carbon sequestration in tidal salt marshes of the northeast United States. *Environmental Management*, *56*(4), 998–1008. https://doi.org/10.1007/s00267-015-0568-z

Duarte, C. M., Dennison, W. C., Orth, R. J. W., & Carruthers, T. J. B. (2008). The charisma of coastal ecosystems: Addressing the imbalance. *Estuaries and Coasts*, *31*(2), 233–238. https://doi.org/10.1007/s12237-008-9038-7

Duarte, C. M., Losada, I. J., Hendriks, I. E., Mazarrasa, I., & Marbà, N. (2013). The role of coastal plant communities for climate change mitigation and adaptation. *Nature Climate Change*, *3*(11), 961–968. https://doi.org/10.1038/nclimate1970

El-Sayed, M. K. (1987). Chemistry of modern sediments in a hypersaline lagoon, north of Jeddah, Red Sea. *Estuarine, Coastal and Shelf Science*, *25*(4), 467–480. https://doi.org/10.1016/0272-7714(87)90038-2

Eyre, B. D., Andersson, A. J., & Cyronak, T. (2014). Benthic coral reef calcium carbonate dissolution in an acidifying ocean. *Nature Climate Change*, *4*(11), 969–976. https://doi.org/10.1038/nclimate2380

Fourqurean, J. W., Duarte, C. M., Kennedy, H., Marbà, N., Holmer, M., Mateo, M. Á., et al. (2012). Seagrass ecosystems as a globally significant carbon stock. *Nature Geoscience*, *5*(7), 505–509. https://doi.org/10.1038/ngeo1477

Ghazanfar, S. A. (2006). Saline and alkaline vegetation of NE Africa and the Arabian Peninsula: An overview. In M. Oztürk, Y. Waisel, M. A. Khan, & G. Görk (Eds.), *Biosaline Agriculture and Salinity Tolerance in Plants* (pp. 101–108). Basel, Switzerland: Birkhaeuser Verlag.

Gonneea, M. E., Paytan, A., & Herrera-Silveira, J. A. (2004). Tracing organic matter sources and carbon burial in mangrove sediments over the past 160 years. *Estuarine, Coastal and Shelf Science*, *61*(2), 211–227. https://doi.org/10.1016/j.ecss.2004.04.015

Green, E. P., & Short, F. (2003). *World atlas of seagrasses*. Berkeley, CA: University of California Press.

Greiner, J. T., McGlathery, K. J., Gunnell, J., & McKee, B. A. (2013). Seagrass restoration enhances "blue carbon" sequestration in coastal waters. *PLoS One*, *8*(8), e72469–e72468. https://doi.org/10.1371/journal.pone.0072469

Hallegatte, S., Green, C., Nicholls, R. J., & Corfee-Morlot, J. (2013). Future flood losses in major coastal cities. *Nature Climate Change*, *3*(9), 802–806. https://doi.org/10.1038/nclimate1979

Hashimoto, T. R., Saintilan, N., & Haberle, S. G. (2006). Mid-Holocene development of mangrove communities featuring Rhizophoraceae and geomorphic change in the Richmond River Estuary, New South Wales, Australia. *Geographical Research*, *44*(1), 63–76. https://doi.org/10.1111/j.1745-5871.2006.00360.x

Hayes, M. A., Jesse, A., Hawke, B., Baldock, J., Tabet, B., Lockington, D., & Lovelock, C. E. (2017). Dynamics of sediment carbon stocks across intertidal wetland habitats of Moreton Bay, Australia. *Global Change Biology*, *23*, 4222–4234. https://doi.org/10.1111/gcb.13722

Hereher, M. E. (2016). Vulnerability assessment of the Saudi Arabian Red Sea coast to climate change. *Environment and Earth Science*, *75*(1), 1–13. https://doi.org/10.1007/s12665-015-4835-3

Howard, J., Hoyt, S., Isensee, K., Pidgeon, E. & Telszewski, M. (2014). Coastal blue carbon: Methods for assessing carbon stocks and emissions factors in mangroves, tidal salt marshes, and seagrass meadows. Conservation International, Intergovernmental Oceanographic Commission of UNESCO, International Union for Conservation of Nature (pp. 1–180). Arlington, VA. https://doi.org/10.2305/IUCN.CH.2015.10.en

James, N. P., Bone, Y., Brown, K. M., & Cheshire, A. (2009). Calcareous epiphyte production in cool-water carbonate seagrass depositional environments—Southern Australia. In P. K. Swart, G. P. Eberli, & J. A. McKenzie (Eds.), *Perspectives in carbonate geology: A tribute to the career of Robert Nathan Ginsburg* (pp. 123–148). West Sussex, UK: Chichester.

Jankowska, E., Michel, L. N., Zaborska, A., & Włodarska-Kowalczuk, M. (2016). Sediment carbon sink in low-density temperate eelgrass meadows (Baltic Sea). *Journal of Geophysical Research: Biogeosciences*, *121*, 2918–2934. https://doi.org/10.1002/2016JG003424

Khalaf, F. I., & Ala, M. (1980). Mineralogy of the recent intertidal muddy sediments of Kuwait-Arabian Gulf. *Marine Geology*, *35*(4), 331–342. https://doi.org/10.1016/0025-3227(80)90124-3

Kirwan, M. L., Temmerman, S., Skeehan, E. E., Guntenspergen, G. R., & Faghe, S. (2016). Overestimation of marsh vulnerability to sea level rise. *Nature Climate Change*, *6*(3), 253–260. https://doi.org/10.1038/nclimate2909

Krishnaswamy, S., Lal, D., Martin, J. M., & Meybeck, M. (1971). Geochronology of lake sediments. *Earth and Planetary Science Letters*, *11*(1-5), 407–414. https://doi.org/10.1016/0012-821X(71)90202-0

Kristensen, E., Bouillon, S., Dittmar, T., & Marchand, C. (2008). Organic carbon dynamics in mangrove ecosystems: A review. *Aquatic Botany*, *89*(2), 201–219. https://doi.org/10.1016/j.aquabot.2007.12.005

Lo Iocano, C., Mateo, M. A., Gràcia, E., Guasch, L., Carbonell, R., Serrano, L., et al. (2008). Very high-resolution seismo-acoustic imaging of seagrass meadows (Mediterranean Sea): Implications for carbon sink estimates. *Geophysical Research Letters*, *35*, L18601. https://doi.org/10.1029/2008GL034773

Macreadie, P. I., Hughes, A. R., & Kimbro, D. L. (2013). Loss of "blue carbon" from coastal salt marshes following habitat disturbance. *PLoS One*, *8*(7), e69244–e69248. https://doi.org/10.1371/journal.pone.0069244

Macreadie, P. I., Serrano, O., Maher, D., Duarte, C., & Beardall, J. (2017). Addressing calcium carbonate cycling in blue carbon accounting. *Limnology and Oceanography Letters*, *2*(6), 195–201. https://doi.org/10.1002/lol2.10052

Macreadie, P. I., Trevathan-Tackett, S. M., Skilbeck, C. G., Sanderman, J., Curlevski, N., Jacobsen, G., & Seymour, J. R. (2015). Losses and recovery of organic carbon from a seagrass ecosystem following disturbance. *Proceedings of the Royal Society B: Biological Sciences*, *282*(1817). https://doi.org/10.1098/rspb.2015.1537

Marbà, N., Arias-Ortiz, A., Masqué, P., Kendrick, G. A., Mazarrasa, I., Bastyan, G. R., et al. (2015). Impact of seagrass loss and subsequent revegetation on carbon sequestration and stocks. *Journal of Ecology*, *103*(2), 296–302. https://doi.org/10.1111/1365-2745.12370

Masqué, P., Sanchez-Cabeza, J. A., Bruach, J. M., Palacios, E., & Canals, M. (2002). Balance and residence times of ^{210}Pb and ^{210}Po in surface waters of the northwestern Mediterranean Sea. *Continental Shelf Research*, *22*(15), 2127–2146. https://doi.org/10.1016/S0278-4343(02)00074-2

Mateo, M. A., Romero, J., Pérez, M., Littler, M. M., & Littler, D. S. (1997). Dynamics of millenary organic deposits resulting from the growth of the Mediterranean seagrass *Posidonia oceanica*. *Estuarine, Coastal and Shelf Science*, *44*(1), 103–110. https://doi.org/10.1006/ecss.1996.0116

Mazarrasa, I., Marbà, N., Lovelock, C. E., Serrano, O., Lavery, P. S., Fourqurean, J. W., et al. (2015). Seagrass meadows as a globally significant carbonate reservoir. *Biogeosciences*, *12*(16), 4993–5003. https://doi.org/10.5194/bg-12-4993-2015

Mckee, K. L., Cahoon, D. R., & Feller, I. C. (2007). Caribbean mangroves adjust to rising sea level through biotic controls on change in sediment elevation. *Global Ecology and Biogeography*, *16*(5), 545–556. https://doi.org/10.1111/j.1466-8238.2007.00317.x

McLeod, E., Chmura, G. L., Bouillon, S., Salm, R., Björk, M., Duarte, C. M., et al. (2011). A blueprint for blue carbon: Toward an improved understanding of the role of vegetated coastal habitats in sequestering CO_2. *Frontiers in Ecology and the Environment*, *9*(10), 552–560. https://doi.org/10.1890/110004

Meyer-Christoffer, A., Becker, A., Finger, P., Rudolf, B., Schneider, U., & Ziese, M. (2015). GPCC Climatology Version 2015 at 0.25°: Monthly Land-Surface Precipitation Climatology for Every Month and the Total Year from Rain-Gauges built on GTS-based and Historic Data. https://doi.org/10.5676/DWD_GPCC/CLIM_M_V2015_025

Miyajima, T., Hori, M., Hamaguchi, M., Shimabukuro, H., Adachi, H., Yamano, H., & Nakaoka, M. (2015). Geographic variability in organic carbon stock and accumulation rate in sediments of East and Southeast Asian seagrass meadows. *Global Biogeochemical Cycles*, *29*, 397–415. https://doi.org/10.1002/2014GB004979

Nellemann, C., Corcoran, E., Duarte, C., Valdés, L., DeYoung, C., Fonseca, L., & Grimsditch, G. (Eds.) (2009). Blue carbon. A rapid response assessment, United Nations Environ. Program., GRID- Arendal. Retrieved from www.grida.no

Neumann, B., Vafeidis, A. T., Zimmermann, J., & Nicholls, R. J. (2015). Future coastal population growth and exposure to sea-level rise and coastal flooding—A global assessment. *PLoS One*, *10*(3), e0118571. https://doi.org/10.1371/journal.pone.0118571

Nittrouer, C. A., DeMaster, D. J., McKee, B. A., Cutshall, N. H., & Larsen, I. L. (1984). The effect of sediment mixing on Pb-210 accumulation rates for the Washington continental shelf. *Marine Geology*, *54*(3-4), 201–221. https://doi.org/10.1016/0025-3227(84)90038-0

Palinkas, C. M., & Koch, E. W. (2012). Sediment accumulation rates and submersed aquatic vegetation (SAV) distributions in the mesohaline Chesapeake Bay, USA. *Estuaries and Coasts*, *35*(6), 1416–1431. https://doi.org/10.1007/s12237-012-9542-7

Pergent, G., Bazairi, H., Bianchi, C. N., Boudouresque, C. F., Buia, M. C., Clabaut, P., et al. (2012). Mediterranean seagrass meadows: Resilience and contribution to climate change mitigation, a short summary / Les herbiers de magnoliophytes marines de Méditerranée: Résilience et contribution à l'atténuation des changements climatiques, Résumé (40 pp.). Gland, Switzerland and Málaga, Spain: IUCN.

Pilkey, O. H., & Noble, D. (1966). Carbonate and clay mineralogy of the Persian Gulf. *Deep-Sea Research*, *13*(1), 1–16. https://doi.org/10.1016/0011-7471(66)90002-7

Poppe, K. L. (2015). An ecogeomorphic model to assess the response of Padilla Bay's eelgrass habitat to sea level rise., WWU Masters Thesis Collection. Paper 458.

Por, F. D., & Dor, I. (1975). The hard bottom mangroves of Sinai, Red Sea. *Rapport et Communication Internationale de la Mer Mediterranean*, *23*(2), 145–147.

Price, A. R. G., Dawson Shepherd, A. R., McDowall, R. J., Stafford Smith, M. G., Ormond, R. F. G., Wrathall, T. J., et al. (1988). Aspects of seagrass ecology along the eastern coast of the Red Sea. *Botanica Marina*, *31*(1), 83–92. https://doi.org/10.1515/botm.1988.31.1.83

Price, A. R. G., Ghazi, S. J., Tkaczynski, P. J., Venkatachalam, A. J., Santillan, A., Pancho, T., et al. (2014). Shifting environmental baselines in the Red Sea. *Marine Pollution Bulletin*, *78*(1–2), 96–101. https://doi.org/10.1016/j.marpolbul.2013.10.055

Price, A. R. G., Medley, P. A. H., McDowall, R. J., Dawson-Shepherd, A. R., Hogarth, P. J., & Ormond, R. F. G. (1987). Aspects of mangal ecology along the Red Sea coast of Saudi Arabia. *Journal of Natural History*, *21*(2), 449–464. https://doi.org/10.1080/00222938700771121

Pugh, D. T., & Abualnaja, Y. (2015). Sea-level changes. In I. C. F. Stewart & N. M. A. Rasul (Eds.), *Red Sea: The formation, morphology, oceanography and environment of a young ocean* (Vol. 18, pp. 317–328). Heildelberg: Berlin.

Reghellin, D., Dickens, G. R., & Backman, J. (2013). The relationship between wet bulk density and carbonate content in sediments from the eastern equatorial Pacific. *Marine Geology*, *344*, 41–52. https://doi.org/10.1016/j.margeo.2013.07.007

Saderne, V., Cusack, M., Almahasheer, H., Serrano, O., Masqué, P., Arias-Ortiz, A. et al. (2018). Sediment characteristics ofdifferent coastal ecosystems along the Central eastern Red Sea coast and western Arabian Gulf, PANGAEA. https://doi.org/10.1594/PANGAEA.887043 (DOI registration in progress)., In supplement to: Saderne, V. et al., Accumulation of carbonates contributes to coastal vegetated ecosystems keeping pace with sea level rise in an arid region (Arabian Peninsula)., J. Geophys. Res. Biogeosciences.

Sanchez-Cabeza, J. A., Masqué, P., & Ani-Ragolta, I. (1998). Lead-210 and polonium-210 analysis in sediments and sediments by microwave acid digestion. *Journal of Radioanalytical and Nuclear Chemistry*, *227*(1-2), 19–22. https://doi.org/10.1007/BF02386425

Sanders, C. J., Maher, D. T., Tait, D. R., Williams, D., Holloway, C., Sippo, J. Z., & Santos, I. R. (2016). Are global mangrove carbon stocks driven by rainfall? *Journal of Geophysical Research: Biogeosciences*, *121*, 2600–2609. https://doi.org/10.1002/2016JG003510

Sanders, C. J., Smoak, J. M., Naidu, A. S., Araripe, D. R., Sanders, L. M., & Patchineelam, S. R. (2010). Mangrove forest sedimentation and its reference to sea level rise, Cananeia, Brazil. *Environment and Earth Science*, *60*(6), 1291–1301. https://doi.org/10.1007/s12665-009-0269-0

Sanders, C. J., Smoak, J. M., Naidu, A. S., & Patchineelam, S. R. (2008). Recent sediment accumulation in a mangrove forest and its relevance to local sea-level rise (Ilha Grande, Brazil). *Journal of Coastal Research*, *24*(242), 533–536. https://doi.org/10.2112/07-0872.1

Sasmito, S. D., Murdiyarso, D., Friess, D. A., & Kurnianto, S. (2016). Can mangroves keep pace with contemporary sea level rise? A global data review. *Wetlands Ecology and Management*, *24*(2), 263–278. https://doi.org/10.1007/s11273-015-9466-7

Serrano, O., Davis, G., Lavery, P. S., Duarte, C. M., Martinez-Cortizas, A., Mateo, M. A., et al. (2016). Reconstruction of centennial-scale fluxes of chemical elements in the Australian coastal environment using seagrass archives. *Science of the Total Environment*, *541*, 883–894. https://doi.org/10.1016/j.scitotenv.2015.09.017

Serrano, O., Lavery, P. S., Masqué, P., Inostroza, K., Bongiovanni, J., & Duarte, C. M. (2016). Seagrass sediments reveal the long-term deterioration of an estuarine ecosystem. *Global Change Biology*, *22*(4), 1523–1531. https://doi.org/10.1111/gcb.13195

Serrano, O., Mateo, M. A., Renom, P., & Julià, R. (2012). Characterization of sediments beneath a *Posidonia oceanica* meadow. *Geoderma*, *185-186*, 26–36. https://doi.org/10.1016/j.geoderma.2012.03.020

Serrano, O., Ricart, A. M., Lavery, P. S., Mateo, M. A., Arias-Ortiz, A., Masqué, P., et al. (2016). Key biogeochemical factors affecting sediment carbon storage in *Posidonia* meadows. *Biogeosciences*, *13*(15), 4581–4594. https://doi.org/10.5194/bg-13-4581-2016

Serrano, O., Ruhon, R., Lavery, P. S., Kendrick, G. A., Hickey, S., Masqué, P., et al. (2016). Impact of mooring activities on carbon stocks in seagrass meadows. *Scientific Reports*, *6*. https://doi.org/10.1038/srep23193

Sheppard, C., Al-Husiani, M., Al-Jamali, F., Al-Yamani, F., Baldwin, R., Bishop, J., et al. (2010). The Gulf: A young sea in decline. *Marine Pollution Bulletin*, *60*(1), 13–38. https://doi.org/10.1016/j.marpolbul.2009.10.017

Societies, S., & April, I. (2016). Blue future. *Nature*, *483*(7391), 509–510. https://doi.org/10.1038/483509a

Sournia, A. (1977). Notes on primary productivity of coastal waters in Gulf of Elat (Red-Sea). *International Review of Der Gesamten Hydrobiology*, *62*(6), 813–819. https://doi.org/10.1002/iroh.1977.3510620606

Southon, J., Kashgarian, M., Fontugne, M., Metivier, B., & Yim, W. W.-S. (2002). Marine reservoir corrections for the Indian Ocean and Southeast Asia. *Radiocarbon*, *44*(01), 167–180. https://doi.org/10.1017/S0033822200064778

Spalding, M., Kainuma, M., & Collins, L. (2010). *World atlas of mangroves (version 1.1). A collaborative project of ITTO, ISME, FAO, UNEP-WCMC, UNESCO-MAB, UNU-INWEH and TNC* (p. 319). London, UK: Earthscan.

Ware, J. R., Smith, S. V., & Reaka-kudla, M. L. (1992). Coral Reefs Coral reefs: sources or sinks of atmospheric CO_2? *Coral Reefs*, *11*, 127–130. https://doi.org/10.1007/bf00255465

Woodroffe, C. D., Rogers, K., McKee, K. L., Lovelock, C. E., Mendelssohn, I. A., & Saintilan, N. (2016). Mangrove sedimentation and response to relative sea-level rise. *Annual Review of Marine Science*, *8*(1). https://doi.org/10.1146/annurev-marine-122414-034025